Muscular Viscoelasticity Design and Evaluation in Feed-forward Position Control of Robot Arm based on Animal Musculoskeletal Model

Kengo Yoshida, Sehoon Oh and Yoichi Hori
Department of Electrical Engineering
School of Engineering
University of Tokyo, 3-7-1
Hongo Bunkyoku Tokyo, Japan
Email:yoshida@horilab.iis.u-tokyo.ac.jp, sehoon@horilab.iis.u-tokyo.ac.jp, hori@iis.u-tokyo.ac.jp

***Abstract*— This paper describes important role of muscular viscoelasticity at Feed-forward position control of robot arm based on animal musculoskeletal model. Feed-back controller of animals has big delay. Therefore, feed-forward (FF) controller contributes mainly in local motor control of animals. We focus control ability of animal muscle. Muscle has variable viscoelasticity according to muscular activation level. Proposed controller utilize this characteristic. The controller based on antagonistic muscular pair can be represented by equivalent block diagram containing PD controller. This representation enables its design and evaluation easily. Proposed controller is evaluated by our experimental robot arm which has a mechanism based on bi-articular muscle.**

I. INTRODUCTION

Recently many industrial robots work in advanced factory. On the other hand, human-cooperative robots are desired in aging society to help people. Industrial robots work separated from human but human-cooperative robots do not. Necessary ability is different in each type of robots. Industrial robots need precise and high speed operation in well-known environment. While human-cooperative robots are not always necessarily such ability. Instead, compliant motion for safety and skillful operation in unknown environment are more important. Latter abilities are advantages of animal over robot. We have intended to introduce animal structure into robot so that human-cooperative robot obtains latter abilities. Especially we focus three characteristics of animal arm: (1)bi-articular driving, (2)antagonistic driving and (3)variable viscoelasticity. Fig. 1 shows difference between animal and robot arm structure.

Bi-articular muscles are ignored in many robotics research, but recently their important role is clarified. Van Ingen Schenau et. al. described a role of bi-articular muscles in vertical jump. Gastrocnemius muscle is a bi-articular muscles in the calf of the leg.It develops and transmits propulsive force [1]. Neville Hogan suggested that antagonistic muscular pair can control position and mechanical impedance. He showed its effectiveness at contact tasks[2][3]. Mussa-Ivaldi verified stiffness ellipse at the end point of human arm in several postures experimentally[4]. Kumamoto and Oshima et. al. suggested modeling of human arms and legs using two antagonistic pairs of mono-articular muscles and one antagonistic pair of bi-articular muscles. They proposed that direction of distal output force is controlled by switching pattern of antagonistic muscular pairs. This pattern is backed by recorded EMG patterns of human upper arm. [5].

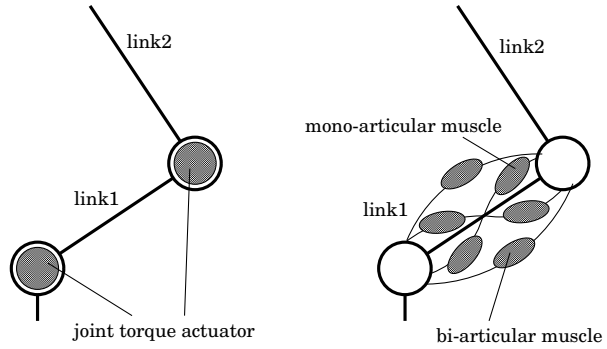

Fig. 1. Conventional robot arm model and animal's arm model

There are several application to utilize musculoskeletal model to verify or utilize control ability of muscles. Kumamoto made experimental machine using pneumatic actuators to verify their theory[5]. Oshima proposed jumping leg robot. They connected knee and ankle joints with wire. The wire is corresponding to gastrocnemius muscles. It contributes to stabilization of posture [6]. Niiyama made jumping frog robot. Their robot imitates frog muscular alignment. However they omit some redundant muscles. Their robot can jump with simple control [7]. Oda and et al. developed unique actuator to mimic muscular viscoelasticity mechanically. They mount this actuators on their robot arm. Also they develops jumping robot leg which has springs as bi-articular muscles.[8] However its performance is limited to static operation or particular action. We intend to clarify control ability of musculoskeletal system in arbitrary movement.

This paper describes important role of muscular viscoelas-

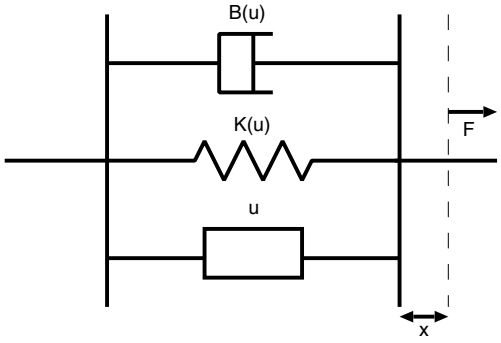

Fig. 2. Model of a muscle

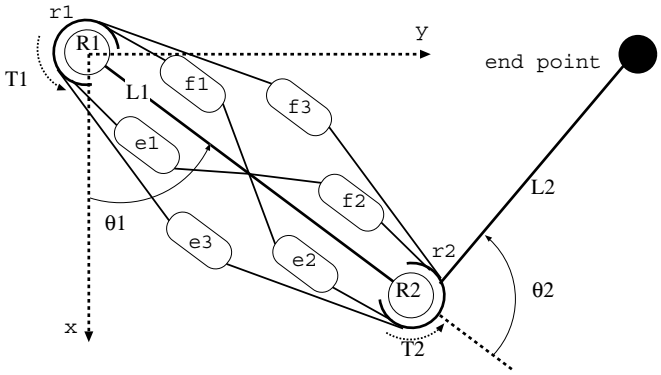

Fig. 3. Two joint link model with both mono-articular muscles and bi-articular muscles

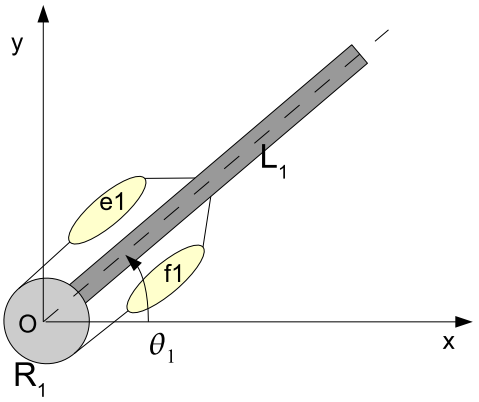

Fig. 4. One joint arm model with antagonistic muscular pair

ticity at Feed-forward position control of robot arm based on animal musculoskeletal model. Section II describes musculoskeletal models of animal arm. Section III shows proposed controller based on antagonistic muscular pair. Then Section IV evaluates proposed controller by both simulation and experiment.

Authors developed a novel robot arm based on bi-articular muscle principle. This robot is used for experimental verification[9]. FF path tracking algorithm is also proposed by authors[10]. This paper extends concept of above algorithm and analyze circumstantially.

II. Musculoskeletal Model

Muscle has unique viscoelasticity. Animal Muscular model is shown in Fig. 2. According to Ito and Tsuji, muscular output force F is a function of contractile force u.[11]

$$F = u - K(u)x - B(u)\dot{x} = u - kux - bu\dot{x} \tag{1}$$

Here x is contracting length of the muscle and $\dot{x}$ is shortening velocity. k is elastic coefficient and b is viscosity coefficient. Contractile force u is only settled actively and others are passive elements. In other word u is assumed as activation level of muscle.

Muscles only generate forces when they shrink. Therefore muscles construct antagonistic pair to generate dual-directional force.

In this paper we use simplified two joint link model shown in Fig. 3. In Fig. 3 e1 and f1 are a pair of antagonistic mono-articular muscles attached to joint R1. e2 and f2 are attached to R2. e3 and f3 are a pair of antagonistic bi-articular muscles attached both R1 and R2.

We define output forces of each muscle as F_{f1}, F_{e1}, F_{f2}, F_{e2}, F_{f3}, and F_{e3}. r_1 and r_2 are radii of R1 and R2. Joint moments T_1 and T_2 are as follows:

$$\begin{aligned} T_1 &= (F_{f1} - F_{e1})r_1 + (F_{f3} - F_{e3})r_1 \\ T_2 &= (F_{f2} - F_{e2})r_2 + (F_{f3} - F_{e3})r_2 \end{aligned} \tag{2}$$

For convenience of calculation, summation and difference of contractile force of antagonistic muscular pair are defined. u_{f1}, u_{e1}, u_{f2}, u_{e2}, u_{f3} and u_{e3} are contractile force in each muscle. Summations S_1, S_2, S_3 and differences D_1, D_2, D_3 are as follows:

$$\begin{aligned} S_1 &= u_{f1} + u_{e1} \quad , \quad D_1 = u_{f1} - u_{e1} \\ S_2 &= u_{f2} + u_{e2} \quad , \quad D_2 = u_{f2} - u_{e2} \\ S_3 &= u_{f3} + u_{e3} \quad , \quad D_3 = u_{f3} - u_{e3} \end{aligned} \tag{3}$$

under the following conditions:

$$|S_1| > |D_1|, |S_2| > |D_2|, |S_3| > |D_3|$$

III. Controller based on antagonistic muscular pair

A. Controller for one joint arm

Fig. 4 shows one joint arm model with antagonistic muscular pair. This model is extracted around R1 joint of Fig. 3. Dynamic equation around R1 joint is shown Eq. (4). J_1 is inertia around R1 joint.

$$J_1\ddot{\theta} = r_1(D_1 - kr_1\theta_1 S_1 - br_1\dot{\theta}_1 S_1)) \tag{4}$$

When constant contractile forces are given, solution of Eq. (4) is calculated as Eq. (5).

$$\theta(t) = Ae^{\alpha t} + Be^{\beta t} + \frac{D_1}{kr_1 S_1} \tag{5}$$

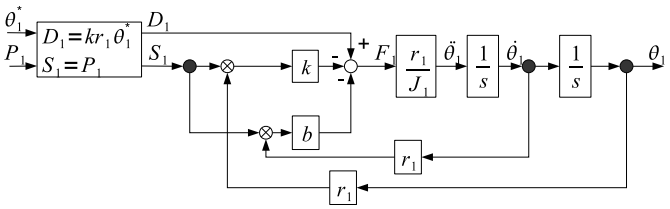

Fig. 5. Block diagram of one joint controller based on antagonistic muscular pair

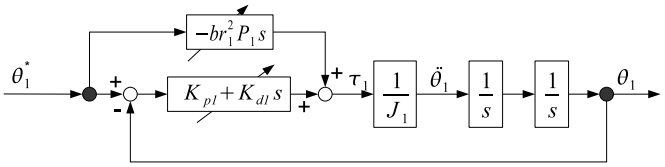

Fig. 6. Equivalent block diagram containing PD controller

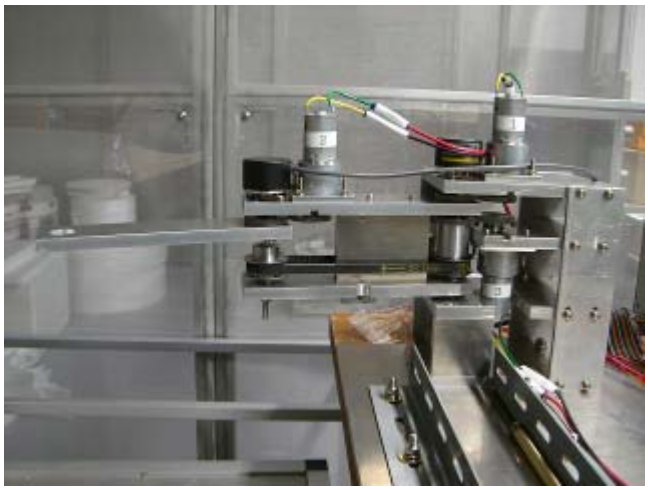

Fig. 7. A photo of robot arm

where:

$$A = \frac{\theta_{1\_0} - \frac{\dot{\theta_1}_{\_0}}{\beta} - \frac{D_1}{kr_1 S_1}}{1 - \frac{\alpha}{\beta}} \quad , \quad \alpha = \frac{-br_1 S_1 + \sqrt{(b^2 r_1^2 S_1 - 4J_1 k)S_1}}{2J_1}$$

$$B = \frac{\theta_{1\_0} - \frac{\dot{\theta_1}_{\_0}}{\alpha} - \frac{D_1}{kr_1 S_1}}{1 - \frac{\beta}{\alpha}} \quad , \quad \beta = \frac{-br_1 S_1 - \sqrt{(b^2 r_1^2 S_1 - 4J_1 k)S_1}}{2J_1}$$

θ_{1_0} is initial angle at $t = 0$. θ_1 converges to D_1/kr_1S_1 except oscillatory solution $b = 0$. To change S_1 and D_1, position and system behavior of one joint arm can be controlled. Fig. 5 is controller of one joint arm based on antagonistic muscular pair. $\theta_1^\star$ is desired angle and P_1 is corresponding to stiffness. Summation and difference of contractile forces are defined using $\theta_1^\star$ and P_1 in Eq. (6).

$$\begin{aligned} S_1 &= P_1 \\ D_1 &= kr_1\theta_1^\star P_1 \end{aligned} \tag{6}$$

In Fig. 5, $\otimes$ means multiplication operator of input values. This muscular controller can be represented equivalent controller containing PD controller as Fig. 6. Parameters of PD controller are shown in Eq. (7).

$$\begin{aligned} K_{p1} &= kr_1^2 P_1 \\ K_{d1} &= br_1^2 P_1 \end{aligned} \tag{7}$$

Eq. (8) represents value of P_1 as indication.

$$P_1 = \frac{4.0kJ_1}{b^2 r_1^2} \tag{8}$$

B. Controller for two joint link arm

Each joint angle is controlled independently by antagonistic muscular pairs in the case without bi-articular muscle. Each joint torque is represented by Eq. (9).

$$\begin{pmatrix} \tau_1 \\ \tau_2 \end{pmatrix} = \begin{pmatrix} r_1(D_1 - kr_1\theta_1 S_1 - br_1\theta_1 S_1) \\ r_2(D_2 - kr_2\theta_2 S_2 - br_2\theta_2 S_2) \end{pmatrix} \tag{9}$$

S_1, S_2, D_1, D_2 are defined as well as controller of one joint arm.

$$\begin{aligned} S_1 = P_1 \quad , \quad D_1 = kr_1\theta_1^\star P_1 \\ S_2 = P_2 \quad , \quad D_2 = kr_2\theta_2^\star P_2 \end{aligned} \tag{10}$$

In the case with bi-articular muscles, Each joint torque is shown by Eq.(11).

$$\begin{pmatrix} \tau_1 \\ \tau_2 \end{pmatrix} = \begin{pmatrix} r_1(D_1 - kr_1\theta_1 S_1 - br_1\theta_1 S_1) + r_1\tau_{pair3} \\ r_2(D_2 - kr_2\theta_2 S_2 - br_2\theta_2 S_2) + r_2\tau_{pair3} \end{pmatrix} \tag{11}$$

where:

$$\tau_{pair3} = D_3 - k(r_1\theta_1 + r_2\theta_2)S_3 - b(r_1\theta_1 + r_2\theta_2)S_3$$

In addition to Eq. (10), contractile force of bi-articular muscles are defined by Eq. (12).

$$S_3 = P_3 \quad , \quad D_3 = k(r_1\theta_1^\star + r_2\theta_2^\star)P_3 \tag{12}$$

Antagonistic pair of bi-articular muscles controls summation of both joint angles.

IV. Verification of Proposed Controller

A. Robot arm based on bi-articular muscle principle

Fig. 7 shows experimental robot arm based on animal musculoskeletal structure. Three important characteristics of animal arm is realized in the robot arm. Each antagonistic muscular pair is replaced by DC motor. Bi-articular muscle is mimicked by pulley and timing belt as bi-articular driving mechanism. Muscular viscoelasticity is emulated by software control. Elastic coefficient k is 3.0 N/m and viscosity coefficient b is 1.0 Ns/m.

Table I shows main properties of the robot arm. These properties are in common with a simulation model. The robot arm is controlled by Art-linux for real-time operation system. Sampling time is 1 msec.

These geared motors have large friction and other nonlinearity. To nominalize these motors, simple disturbance observer is used. Nominal parameters are same with TABLE I. Cut off

TABLE I
PROPERTIES OF ROBOT ARM

Total height	270mm
Total length	500mm
Total mass of link 1	0.72kg
Total Length of link 1 between joint 1 and 2	165mm
Total mass of link 2	0.27kg
Total length of link 2 between joint 2 and center of force sensor	185mm
Moment of inertia of joint 1	0.034kg·m^2
Moment of inertia of joint 2	0.0058kg·m^2
Torque coefficient	0.20Nm/A

frequency is 100Hz. Also simple compensator of static friciton is added. When absolute value of angular speed is less than 0.0001, 0.12Nm of torque is added as compensation of static friction force.

B. Verification of one joint arm controller

Firstly proposed controller for one joint arm is verified. In each simulation and experiment, square wave is given as position command. Amplitude of the wave is 0.3 rad.

Fig. 8 are simulation results of changing P_1. This is equals to changing summation of contractile force as stiffness of the joint. Overlarge stiffness prevent quick movement. However too small stiffness cause overshoot of the arm. Fig. 9 are experimental results. In actual experiment, the case of small stiffness ($P_1 = 10$) is more unstable than in simulation result.

In Fig. 10, to evaluate robustness against model disturbance, the arm has a load at the end point. The mass of load $m_{load}$is changed for the two cases which are different in summation of contractile force. Experimental results are shown in Fig. 11. A value of P_1 derived from Eq. (8) indicates good performance in both quick response and robustness.

C. Verification of two joint arm controller

Then proposed controller for two link arm is verified. Fig. 12 shows simulation results. Summation of contractile forces are calculated by Eq. (8). In the case without bi-articular muscle, each joint is controlled independently but it has large overshoot. While in the case with bi-articular muscle, responses are improved. Bi-articular muscle controls summation of both joint angles and it contributes to suppress position error in working space.

V. CONCLUSION

This paper proposed FF position controller based on antagonistic muscular pair. We showed equivalent block diagram containing PD controller in order to represent characteristic of proposed controller. Simulation and experimental result verified performance and robustness of proposed controller.

Antagonistic driving by actuator which has variable viscoelasticity can make mechanical impedance. Furthermore, adding bi-articular driving distal mechanical impedance can be controlled independently from distal output. This characteristic contributes safety at collision. Our proposed controller is suitable for the robot based on animal musculoskeletal system.

REFERENCES

[1] G. J. van Ingen Shenau, M. F. Bobbert and R. H. Rozendal, "The unique action of bi-articular muscles in complex movements", Journal of Anatomy, 155, pp. 1-5, 1987

[2] Neville Hogan, "Adaptive Control of Mechanical Impedance by Coactivation of Antagonist Muscles", IEEE Transactions on Automatic Control, vol.AC-29, No.8, pp. 681-690, 1984

[3] Neville Hogan, "On the stability of Manipulators Performing Contact Tasks", IEEE Journal of Robotics and Automation, Vol. 4, No. 6, pp. 677-686, 1988

[4] F. A. Mussa Ivaldi, N. Hogan and E. Bizzi, "Neural, Mechanical, and Geometric Factors Subserving Arm Posture in Humans", The Journal of Neuroscience, Vol. 5, No. 10, pp. 2732-2743, 1985

[5] Mizuyori Kumamoto, Toru Oshima, Tomohisa Yamamoto, "Control properties induced by existence of antagonistic pairs of bi-articular muscles -Mechanical engineering model analyses", Human Movement Science 13, pp. 611-634, 1994

[6] Toru Oshima, Noboru Momose and Kiyoshi Toriumi, "Jump mechanism using coordination in knee and ankle joint and application to leg orthosis" , The 2005 International Power Electronics Conference, 2005

[7] Ryuma Niiyama, Akihiko Nagakubo, Yasuo Kuniyoshi, "A bipedal jumping and landing robot with an artificial musculoskeletal system", IEEE International Conference on Robotics and Automation, 2007

[8] Mizuyori Kumamoto and et al., "Revolution in Humanoid Robotics", Tokyo Denki University Press, 2006 (in Japanese)

[9] Kengo Yoshida, Toshiyuki Uchida, Sehoon Oh and Yoichi Hori, "Experimental Verification on Novel Robot Arm Equipped with Bi-articular Driving Mechanism", IEEE ISIE 2009, 2009. Korea

[10] Kengo Yoshida, Naoki Hata, Toshiyuki Uchida and Yoichi Hori, "Novel FF Control Algorithm of Robot Arm Based on Bi-articular Muscle Principle - Emulation of Muscular Viscoelasticity for Disturbance Suppression and Path Tracking", IEEE IECON 2007, 2007, Taiwan

[11] K. Ito and T. Tsuji, "The bilinear characteristics of Muscle-Skeletomotor system and the application to prosthesis control", The Transactions of the Electrical Engineers of Japan 105-C(10), pp. 201-208, 1985

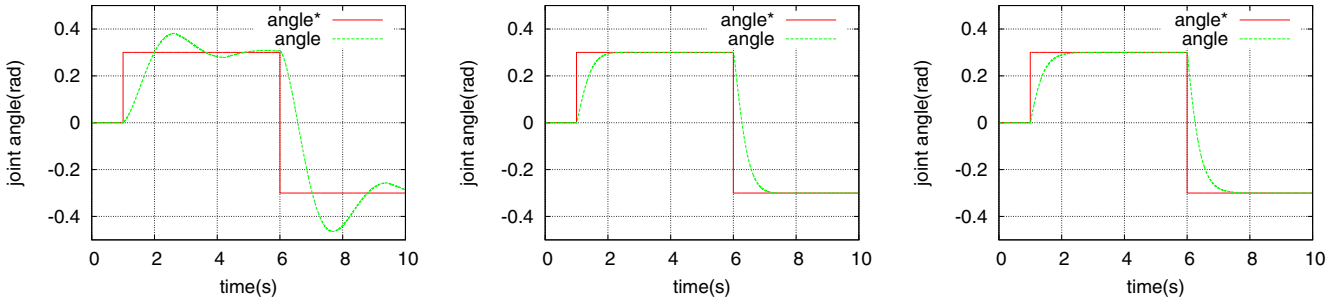

$P_1 = 10$ $P_1 = 90$ derived from Eq.(8) $P_1 = 150$

Fig. 8. Simulation results of changing P_1

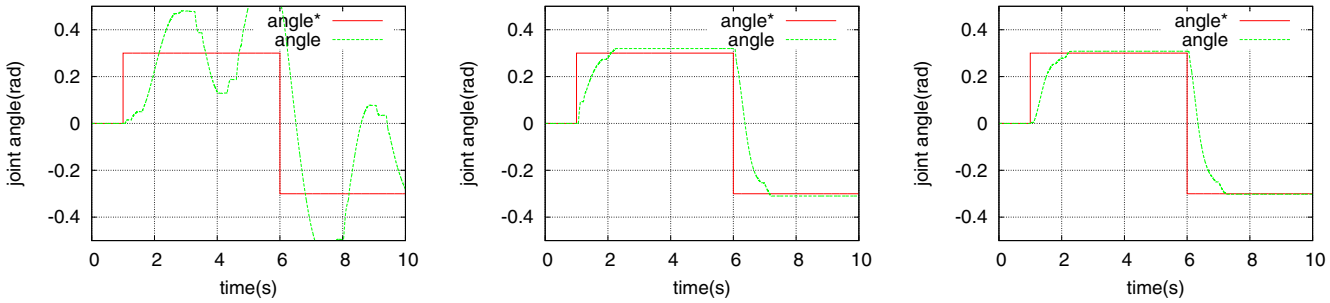

$P_1 = 10$ $P_1 = 90$ derived from Eq.(8) $P_1 = 150$

Fig. 9. Experimental results of changing P_1

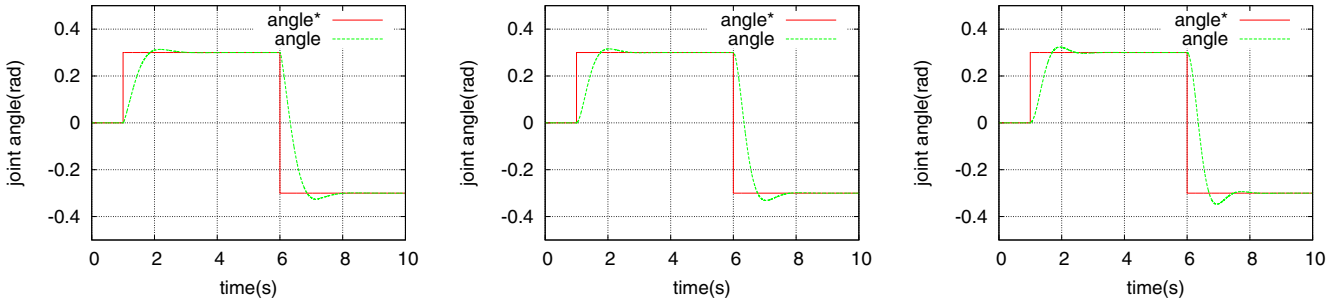

$m_{load} = 0$[kg] $m_{load} = 0.15$[kg] $m_{load} = 0.3$[kg]

case 1 : $P_1 = 40$

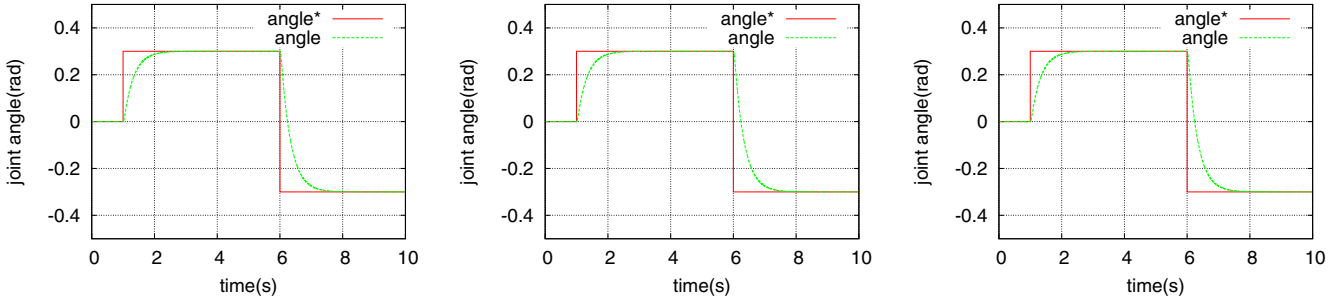

$m_{load} = 0$[kg] $m_{load} = 0.15$[kg] $m_{load} = 0.3$[kg]

case 2 : $P_1 = 90$, derived from Eq.(8)

Fig. 10. Simulation results of changing mass of the load

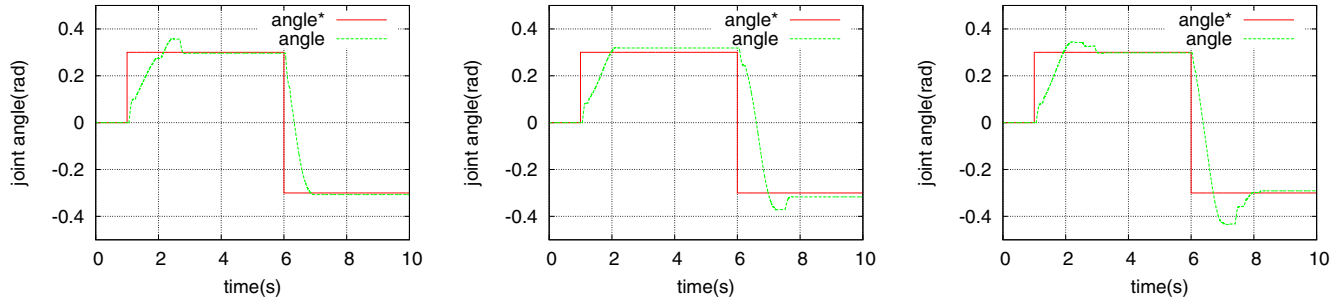

$m_{load} = 0$[kg] $m_{load} = 0.15$[kg] $m_{load} = 0.3$[kg]

case 1 : $P_1 = 40$

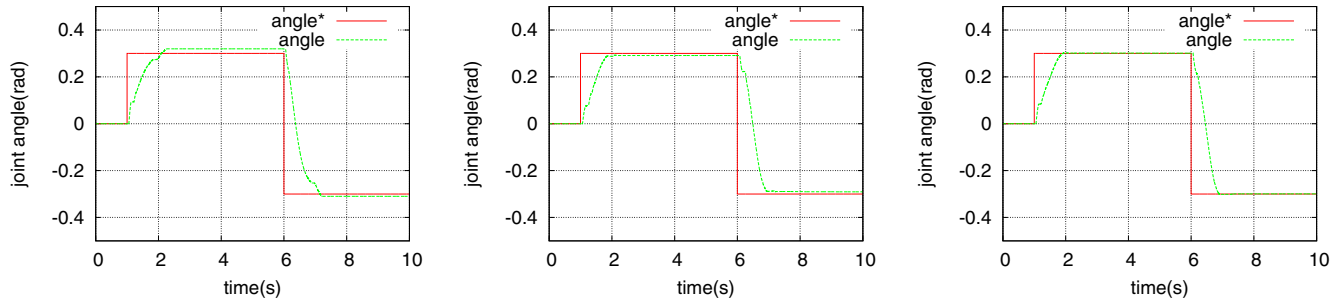

$m_{load} = 0$[kg] $m_{load} = 0.15$[kg] $m_{load} = 0.3$[kg]

case 2 : $P_1 = 90$, derived from Eq.(8)

Fig. 11. Experimental results of changing mass of the load

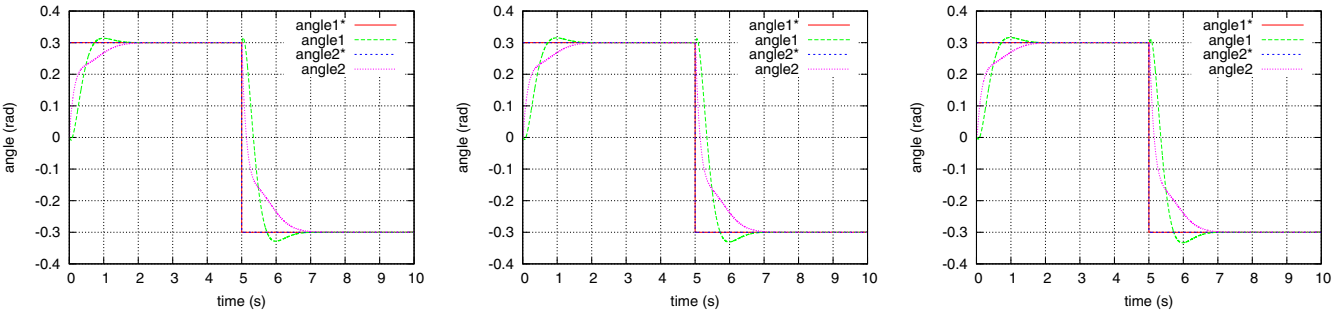

$m_{load} = 0$[kg] $m_{load} = 0.05$[kg] $m_{load} = 0.1$[kg]

with bi-articular muscle

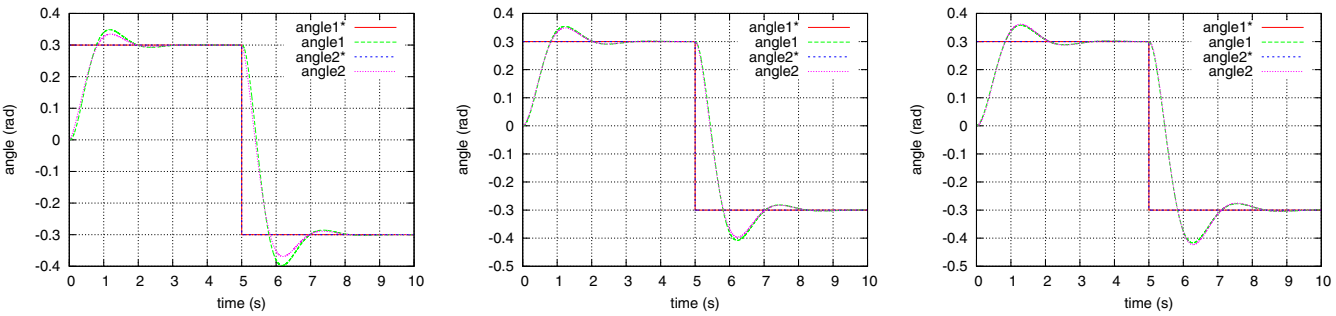

$m_{load} = 0$[kg] $m_{load} = 0.05$[kg] $m_{load} = 0.1$[kg]

without bi-articular muscle

Fig. 12. Simulation results of two joint arm controller